

promoting access to White Rose research papers



Universities of Leeds, Sheffield and York
<http://eprints.whiterose.ac.uk/>

This is the author's version of an article published in **Bioresource Technology**

White Rose Research Online URL for this paper:

<http://eprints.whiterose.ac.uk/id/eprint/75970>

Published article:

Pimenidou, P, Rickett, G, Dupont, V and Twigg, MV (2010) *Chemical looping reforming of waste cooking oil in packed bed reactor*. *Bioresource Technology*, 101 (16). 6389 - 6397. ISSN 0960-8524

<http://dx.doi.org/10.1016/j.biortech.2010.03.053>

Chemical looping reforming of waste cooking oil in packed bed reactor

P. Pimenidou¹, G. Rickett¹, V. Dupont^{1*}, M. V. Twigg²

¹*Energy and Resources Research Institute, The University of Leeds, Leeds LS2 9JT, UK*

²*Johnson Matthey Orchard Laboratory, Orchard Road, Royston, SG8 5HE, UK*

Corresponding author: V.Dupont@leeds.ac.uk

Paper accepted and published. Full reference:

Pimenidou, P., Rickett, G. L., Dupont, V, Twigg, M. V. Chemical looping reforming of waste cooking oil in packed bed reactor. *Bioresource Technology* 101 (2010) 6389–6397.

Abstract

Chemical looping steam reforming for hydrogen production from waste cooking oil was investigated using a packed bed reactor. The steam to carbon ratio of 4 and temperatures between 600 and 700 °C yielded the best results of the range of conditions tested. Six cycles at two weighted hourly space velocities (WHSV of 2.64 and 5.28 hr⁻¹) yielded high (>0.74) and low (<0.2) oil conversion fractions respectively, representing low and high coking conditions. The WHSV of 2.64 hr⁻¹ yielded product concentrations closest to equilibrium values calculated assuming a fresh rapeseed oil composition. Repeated cycling revealed some output oscillations in reactant conversion and in the extent of Ni-NiO conversion, but did not exhibit deterioration by the 6th cycle. The selectivity of CO, CO₂ and CH₄ were remarkably constant over the performed cycles, resulting in a repeatable syngas composition with H₂ selectivity very close to the optimum.

Keywords: chemical looping, reforming, waste oil, nickel, hydrogen

1 Introduction

Global efforts in reducing greenhouse gas emissions have spurred intense research in sustainable production methods of biofuels and hydrogen. While the catalytic transesterification of vegetable oils for the production of fatty acid methyl esters (FAME) has been optimized for fresh vegetable oil feedstocks, used oils such as waste cooking oils present a number of challenges in addition to being unfit for human and animal consumption. They have a higher content in moisture and free fatty acids (FFA) caused by the hydrolysis of the triglycerides during the cooking of moist food (O.R. Fennema, 1985). The alkaline catalysts in the transesterification process are unable to convert FFAs due to the formation of soap (fatty acid salts), which in turn prevent phase separation of the FAME from the crude glycerol fraction (Canacki, 2007). Although acid catalysts are able to esterify free fatty acids, the process generates water as a by-product and a two-stage process may be necessary (Canacki, 2003). Oxidation stability is also reduced compared to the fresh oil by the contact of hot oil with food, yielding a higher peroxide value (Tomasevic and Siler-Marinkovic, 2003). Higher values of saponification, density and viscosity, are attained, the latter due to the formation of dimeric and polymeric acids and glycerides (Chang et al, 1978). A higher bromine index has also been reported, as well as an increased polarity with repeated frying (Bezergianni et al, 2009). When used in diesel engines, waste cooking oils can also yield increased NO_x emissions (Bezergianni et al, 2009). Used cooking oils usually exhibit a decrease in molar mass and iodine value compared to fresh oils. Due to the difficulties in using waste cooking oils for biodiesel production, it is worth considering this significant waste stream as a potential source of renewable hydrogen. Investigations into the thermal cracking and the steam gasification or reforming of vegetable oils have appeared regularly in the literature since the mid-1980s (e.g. Prasad and Bakhshi, 1985, Marquevich et al., 2000 &

2001, Czernik et al., 2004, Maher and Bressler, 2007, Gornay et al, in press). In addition to the obvious energy penalty associated with the endothermicity of the steam gasification reaction, a recurrent problem is the gradual build up of carbon deposits on the solid catalysts. The unmixed steam reforming process (Kumar et al., 1999, Lyon and Cole, 2000) as well as the use of in-situ CO₂ sorption within the reformer, have shown that a nearly pure hydrogen stream can be generated by cycling feed flows in a single reactor, effectively carrying out chemical looping reforming in a packed bed reactor. Methane and vegetable oil have been tested successfully, allowing conditions of high reactants conversion without coking to be identified (Dupont et al., 2007, 2008), whereas the feasibility of sorption enhanced steam reforming of glycerol has been demonstrated (Dou et al., 2009, Chen et al., 2009). Unmixed steam reforming makes use of the chemical looping of an oxygen transfer material (OTM), which in its reduced form also acts as a steam reforming catalyst. Oxidation of the reduced catalyst under air feed allows the separation of N₂ and introduces ‘unmixed combustion’ (Lyon and Cole, 2000) as a means to operate near autothermally, that is, with reduced or little heat input. The carbon formed under the reducing conditions of the fuel/steam feed can also oxidise under air feed. A crucial requirement of the chemical looping process is the ability of the fuel to carry out the reduction and oxidation of the OTM repeatedly. The present study investigates unmixed steam reforming of waste vegetable cooking oil with only the OTM catalyst present, and not the CO₂ sorbent, to determine the suitability of this challenging fuel to maintain steam reforming activity under chemical looping reforming conditions. A forthcoming publication will focus on the same fuel and process with in-situ CO₂ capture, an additional form of chemical looping, thereby producing a high H₂ purity syngas.

2 Materials and Methods

2.1 Materials

Previous studies have been dedicated to the screening and selection of catalysts and CO₂ sorbents for unmixed steam reforming (Dupont et al, 2007). The OTM catalyst chosen here had 18 wt % NiO supported on Al₂O₃ originally in a pellet form. The pellets were crushed and sieved to give a particle size distribution range of 0.85 to 2 mm in diameter. Sample masses of 40 g or 80 g of fresh catalyst were weighed and loaded into the reactor so that the catalyst was at the centre of the heated zone. A plug 25 mm thick of spherical Al₂O₃ beads was placed below the catalyst to hold it in place.

The waste cooking vegetable oil (WCO) came from the University of Leeds' refectory and had a liquid density of 920 kg m⁻³ at 20 °C. An average gross calorific value of 39.5 MJ kg⁻¹ was determined using a 6200 Oxygen Bomb Calorimeter from Parr Instrument Co. CHN analysis using a CE Instrument Flash EA 1112 Series measured elemental mass fractions of 74.9±2.5 wt% for carbon, 12.85±1.0 wt% for hydrogen, 0.1±0.01wt% for nitrogen. By difference to 100% and neglecting the sulphur content, this yielded 12.15±1.9 wt% for oxygen. These elemental mass fractions were converted to an average elemental molar formula of C_{0.316}H_{0.645}O_{0.0385}. Given the triglyceride source, the latter can also be expressed as 3(CH_{1.67} + C₁₈H_{37.1}O_{2.31}), where 'CH_{1.67}' represents the portion of glycerol 'backbone' molecule per fatty acid chain, and where the 'C₁₈' fatty acid chain is chosen to reflect the rapeseed oil origin of the WCO used here. As the oxygen mol fraction of 2.31 exceeded the expected mol fraction of 2 of the virgin vegetable fatty acid chains, this confirmed the increased polarity of the waste oil compared to that of the virgin rapeseed oil.

Thermogravimetric analysis of the WCO in N₂ flow (50 cm³ min⁻¹) under a 3 K min⁻¹ heating rate using a Stanton Redcroft TGH1000 TGA indicated a fast and monotonic main stage of mass loss which initiated at a temperature ca. 270 °C, ending just below 400 °C, and

responsible for 80% of the WCO mass loss. A much slower decomposition rate followed, which left 1.84 wt% of residue at 600 °C.

2.2 Bench scale reactor setup

The experiments were carried out in a bench scale reactor set up as shown in figure 1. The mass flow rates of air, nitrogen and hydrogen were regulated by three MKS mass flow controllers. The mass flow rates of used cooking oil and water were regulated by two peristaltic pumps and then passed through two separate pre-heaters. They entered the reactor as vapour by means of two co-axial injectors with steam on the inside. The preheat temperature for the water steam was set at 130 °C to avoid film boiling and maximising heat transfer. Based on the TGA results, the preheat temperature of 300 °C was selected to bring the WCO as close as possible to vapourisation, but stopping short of thermal decomposition to avoid tar formation prior to contacting the catalyst. The temperature of the main reactor and the two pre-heaters were regulated by three Eurotherm temperature controllers with closed loop burst firing. The feed streams of the H₂, N₂, and air gases entering the reactor at the different stages of the process were controlled by solenoid valves switched manually. Three sheathed type K thermocouples (0.5 mm OD) measured the temperature along the reactor's length. The one located in the centre controlled the temperature of the reformer and the other two were at 5 cm above and below the centre respectively, referred to as 'T_{mid}', 'T_{high}' and 'T_{low}'. The product gas leaving the reactor passed through a series of ABB Advanced optima analysers gases analysers via water traps. The main dry gases were measured online every 5 seconds. Concentrations of CO, CO₂ and CH₄ were measured by a Uras 14 infrared absorption analyser, H₂ was monitored with a Caldos 15 thermal conductivity analyser, and O₂ was measured using a Magnos 106 paramagnetic susceptibility analyser. Because other carbon products may have been present, off-line gas chromatography

was carried out after periodically collecting product gas samples in a Tedlar bag. For hydrocarbons from C₁ to C₄, a Varian 3380 gas chromatograph with a flame ionisation detector (GC/FID) was used with N₂ as a carrier gas and with a 2 m length × 2 mm diameter column packed with 80-100 mesh Haysep material.

2.3 Experimental procedures

-Pre-reduction step:

After the fresh catalyst was loaded into the reactor, it was reduced at 700 °C in a 25 % H₂ in N₂ flow of 800 cm³ min⁻¹ STP. As the NiO reduced by converting the H₂ into H₂O, reduction activity was evidenced by concentrations in H₂ of less than 25%. As the NiO reduced, the presence of 25 % H₂ in the exit stream signified the end of the reduction step and the flow of H₂ was then stopped.

-WCO/steam/N₂ feed:

The reactor temperature was then set (600 or 700 °C) and the catalyst was allowed to reach operating temperature under a flow of nitrogen of 600 cm³ min⁻¹ STP. WCO and water were then added simultaneously to the N₂ feed flow. Three liquid feed flow rates at 20 °C were investigated for a single cycle using a 80 g catalyst load: (i) 0.56 cm³ min⁻¹ WCO with 1 cm³ min⁻¹ water, achieving a ‘fuel-rich’ steam to carbon (S:C) ratio of 1.73 with a WHSV (weighted hourly space velocity) of 1.660 hr⁻¹, (ii) 0.55 cm³ min⁻¹ WCO with 1.42 cm³ min⁻¹ water, and (iii) 0.55 cm³ min⁻¹ WCO with 2.32 cm³ min⁻¹ water, yielding ‘excess-steam’ S:C ratios of 2.5, at WHSV of 1.967 hr⁻¹ and of 4, at WHSV of 2.640 hr⁻¹ respectively. The catalyst mass reactor loads of 40 and 80 g were investigated in the chemical looping experiments for 6 cycles each, corresponding to WSHV of 2.64 and 5.28 hr⁻¹ respectively. The stoichiometric S:C was 1.878. The WCO/steam/N₂ feeds lasted in average 67 min, with the shortest duration of 37 min for the 12 cycles tested.

-N₂ purge:

After each WCO/steam/N₂ feed, the WCO and steam pumps were stopped and N₂ flow alone with the same rate of 600 cm³ min⁻¹ (STP) was used to purge the gas products until no residual syngas species were measured at the analysers. This N₂ purge typically lasted 20 min. Then the N₂ flow was stopped.

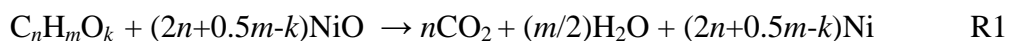
-Air feed:

An air feed of 2000 cm³ min⁻¹ STP then followed the N₂ purge. The air feed durations averaged 28 min for the 12 cycles, with the shortest feed duration of 17 min. The air feed was stopped when the oxygen concentration, having typically measured 0 % or near 0 % in the products from the beginning of the feed, had returned to 21%, indicating no further oxidation reactions were taking place. An air feed was followed by a WCO/steam/N₂ feed, as described earlier.

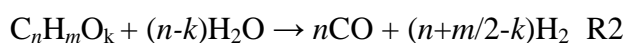
2.4 Reactions and elemental balances

In the absence of the CO₂ sorbent, the following reactions made up the process under the two reactive types of feed.

-Fuel and steam feed:



R1 is a global reaction that illustrates the potential of the fuel to reduce the metal oxide in the OTM. The reduction potential of C_nH_mO_k is therefore 2n+0.5m-k mol of NiO as indicated by R1. It is thus clear that both the carbon and hydrogen content play a role in the OTM reduction, while the O content in the fuel hampers this reaction. While NiO undergoes reduction to Ni, significant coking occurs from fuel thermal decomposition reactions. Once Ni has sufficiently reduced, steam reforming occurs on the Ni-catalyst:



and water gas shift takes place:



The analysers measured the exit dry gas mol (vol) fractions ‘ y_i ’ of CH₄, CO, CO₂, O₂ and H₂.

y_{N_2} was calculated by balance to 1. The total dry molar flow rate leaving the reactor $\dot{n}_{out,dry}$ was determined via a nitrogen balance. The rate of formation \dot{n}_i (e.g. in mol/s) of a particular dry gas product ‘ i ’ could then be calculated using the product of its dry mol fraction with $\dot{n}_{out,dry}$. The carbon balance allowed the calculation of the waste cooking oil conversion fraction X_{WCO} :

$$X_{WCO} = \frac{\dot{n}_{WCO,in} - \dot{n}_{WCO,out}}{\dot{n}_{WCO,in}} = \frac{\dot{n}_{out,dry} (y_{CH_4} + y_{CO} + y_{CO_2})}{n \times \dot{n}_{WCO,in}} \quad (1)$$

Where n was the mol number of atomic C in the WCO elemental formula. Carbonaceous deposits and other carbon products were therefore not taken into account in this fractional fuel conversion calculation. It is therefore assumed that conversions lower than 1 would yield significant carbon deposits. In addition, the N₂ feed is expected to have contained some O₂ impurities (typically 20 ppmv), but the effect of the O₂ impurity on the carbon balance was verified as being negligible. A hydrogen balance yielded an estimate of the fractional steam conversion:

$$X_{H_2O} = \frac{1}{2\dot{n}_{H_2O,in}} \times \left[\dot{n}_{out,dry} (4y_{CH_4} + 2y_{H_2}) - m(\dot{n}_{WCO,in} X_{WCO}) \right] \quad (2)$$

Where m was the mol number of atomic H in the WCO elemental formula.

The rate of NiO reduction to Ni was estimated via the oxygen balance:

$$\dot{n}_{NiO \rightarrow Ni} = \dot{n}_{out,dry} (y_{CO} + 2y_{CO_2} + 2y_{O_2}) - (\dot{n}_{H_2O,in} X_{H_2O}) - k(\dot{n}_{WCO,in} X_{WCO}) \quad (3)$$

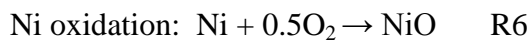
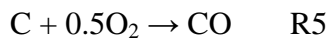
Where k was the mol number of atomic oxygen in the WCO elemental formula.

During each experiment, the exit gas concentrations were recorded every 5 seconds, allowing the above rate equation to be integrated and yield the total number of moles of NiO reduced to Ni over a given period of time. The extent of NiO conversion to Ni was then presented as a percentage of the initial moles of Ni present in the catalyst as reactor load, called ‘extent of NiO→Ni conversion’.

-Air feed step

The reactions under air feed are listed below.

Gasification of the carbonaceous deposits:



In the above process, reactions R1 and 2 are endothermic, while R3-6 are exothermic, the aim being to achieve a cyclic process as close to autothermal as possible.

As before, the nitrogen balance yielded an estimate of the dry gas molar output flow rate

$\dot{n}_{out,dry}$. The carbon balance provided the rate at which the carbon that had deposited under the previous fuel/steam feed underwent partial oxidation to CO or burned completely to CO₂ on the catalyst surface:

$$\dot{n}_{C,oxid} = \dot{n}_{out,dry} \times (y_{CO} + y_{CO_2}) \quad (4)$$

The oxygen balance then yielded $\dot{n}_{Ni \rightarrow NiO}$, the rate of Ni oxidation to NiO deep in the catalyst:

$$\dot{n}_{Ni \rightarrow NiO} = 2\dot{n}_{O_2,in} - \dot{n}_{out,dry} \times (2y_{O_2} + y_{CO} + 2y_{CO_2}) \quad (5)$$

The above equation was then integrated over the duration of the air feed to calculate the total number of moles of Ni oxidised to NiO, and the extent of Ni oxidation to NiO was presented as a % of the total mol of Ni present in the reactor. Note that the effect of impurities in the air

feed such as 400 ppmv of CO₂, was calculated to represent only 0.2% of the oxygen input and to have negligible effect on the outputs of Eqs. 4 and 5.

2.5 Thermodynamic equilibrium calculations.

Thermodynamic calculations were undertaken to compare the experimental outputs with predicted equilibrium values. The computation software used was EQUIL (Lutz et al, 1999, Kee et al, 1980), a FORTRAN program that is part of the suite of the CHEMKIN software. The calculations included the species CO₂, O₂, H₂O, N₂, NH₃, NH₂, CO, H₂, C₁₆H₃₂O₂ (palmitic), C₁₈H₃₆O₂ (stearic), C₁₈H₃₄O₂ (oleic), C₁₈H₃₂O₂ (linoleic), C₁₈H₃₀O₂ (linolenic), CH₄, C₂H₆, C₂H₅, C₂H₄, C₂H₂, C₃H₈, C₃H₇, C₃H₆, C₃H₅, as potential equilibrium products. They were performed for atmospheric pressure at the mid-reactor temperature measured in the experiments. The polynomials of temperature of the specific heat, enthalpy and entropy of the fatty acids, required as programme inputs, were fitted from the data reported in Osmont *et al.* (2007). The latter were derived from quantum chemistry theory using the anharmonic oscillator approximation. The equilibria of steam reforming of oleic, linoleic, linolenic, palmitic and stearic acids were calculated, in addition to a representative mixture of these five fatty acids for an average virgin rapeseed oil. The assumed composition in fatty acids of this representative mixture was 62.5 wt% oleic, 17.8 wt% linoleic, 9.13 wt% linolenic, 4.5 wt% palmitic and 1.74 wt% stearic, and was taken from Eder and Brandsch (2002). Calculated steam conversions and carbon products selectivity showed that they were not sensitive to small changes in the composition, and therefore deviations of our waste cooking oil's composition to that of the assumed virgin rapeseed oil were unlikely to impact greatly on the results. An additional parameter termed 'H₂ purity yield' or $\eta_{H_2, pur}$ defined as:

$$\eta_{H_2, pur} = 100 \times \frac{\text{measured } y_{H_2} \text{ corrected for zero } N_2}{\text{equilibrium } y_{H_2} \text{ corrected for zero } N_2} \quad (6)$$

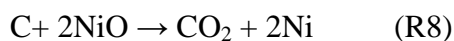
was then used to represent how close the experimental H₂ purity was to the optimum .

3 Results and discussion

3.1 *Effect of steam to carbon ratio*

To find the optimum conditions for unmixed steam reforming of WCO, the effects of steam to carbon ratio on the process outputs of WCO and steam conversions were investigated starting the WCO/steam/N₂ feeds from firstly, the H₂-reduced catalyst, and secondly, the same catalyst previously fully oxidised under air flow. The reduction and oxidation were carried out as previously outlined in 2.3. The reactor temperature was set at 700 °C for these experiments. The steam to carbon ratio of 1.73 is referred to as ‘steam-lean’, while those of 2.5 and 4 are ‘excess-steam’. Table 1 lists the reactants conversions achieved at steady state for the six experiments, alongside the calculated equilibrium values assuming the virgin rapeseed oil composition given in 2.5. The molar production rates of the gaseous products CO, CO₂, CH₄ and H₂ are also included in Table 1. The results indicate that conditions were far from equilibrium for the steam-lean S:C, with very poor experimental WCO and steam conversions. As the S:C increased within the excess-steam range (2.5 to 4), they got closer to the equilibrium values. According to the equilibrium calculations, and as expected, steam conversion decreased as the S:C increased, but did not reach 1 even under steam-lean conditions, due to the reverse water gas shift reaction which is significant at 700 °C. In contrast, the calculated equilibrium WCO conversion remained unchanged at one. In the experiments however, both the WCO and steam conversions were the highest for S:C = 4, and therefore this condition was identified as suitable for the subsequent cycling study in chemical looping conditions. The generation of steam being very energy intensive, the

lowest possible S:C ratio without lowering the process efficiency is desirable. Comparing the steady-state results on the reduced catalyst with those on the oxidised catalyst, it can be seen that they were not that dissimilar. NiO is well known for being inactive in the catalytic steam reforming of hydrocarbons. Here it is shown that vapourised waste cooking oil is able to reduce the catalyst, resulting in triggering and maintaining a steady state in catalytic steam reforming. Furthermore, starting from an oxidised catalyst, the fuel and steam conversions were of similar magnitude as those obtained over the pre-reduced catalyst with hydrogen. The potential for chemical looping of the catalyst using waste cooking oil therefore exists. There were nevertheless some differences between the conversions obtained over the reduced and oxidised catalysts. Surprisingly, for the steam-lean S:C, both the WCO and the steam conversions were significantly higher at steady state starting from the oxidised catalyst compared to starting from the H₂-reduced catalyst. This is explained by the reduced catalyst being conducive to carbon deposition in fuel rich conditions. With the excess of fuel of S:C 1.73, a large conversion to carbonaceous deposits would have occurred, which was observed visually, and evidenced by the evolution of CO and CO₂ under the following air feed. This resulted in low fuel conversions to gaseous carbon containing products. On the other hand, starting from the oxidised catalyst in steam-lean conditions, the carbon would have deposited on NiO and may have partly undergone the reactions below:



Reaction 7 would have increased the measured fuel conversion by generating the gaseous carbon product CO, as well as the steam conversion by favouring the water gas shift reaction, resulting also in higher CO₂. Unfortunately the data was not monitored during the N₂ purge for the present experiments, however during the N₂ purge of the subsequent experiments of WCO chemical looping reforming with sorbent, evidence of CO and CO₂ evolution in excess

of the volumes physically stored in the reactor and pre-analysers pipes was found. This CO₂ could not have been caused by the sorbent decarbonation, as the reactor temperature of ca. 600 °C favoured the carbonation reaction. Further indication of R7 and R8 at work was found by C and O balances over full cycles (including the N₂ purge) when using methane as the fuel (Dupont et al, 2008).

3.2 Chemical looping reforming

Two sets of chemical looping reforming experiments were performed, one using 80 g of catalyst reactor loading, the other using 40 g, resulting in WHSVs of 2.64 and 5.28 hr⁻¹ respectively. Each set started from a H₂-reduced catalyst load. The cycles then comprised a fuel/steam/N₂ feed step, followed by a purge period under N₂ flow feed, and a final air feed step which closed the redox looping of the catalyst. It is worth noting that during the N₂ purge, which is assumed to be a chemically inert step compared to the fuel/steam/N₂ and the air feeds, some Ni reduction and C removal through reactions R7 and R8 could have occurred, while some Ni and C oxidation due to small O₂ impurities in the N₂ flow (20 ppm of O₂ may contaminate the N₂ flow according to the gas manufacturer specification) may also have played a smaller role. This was repeated 6 times so that 12 reactive steps were carried out, 6 in highly reductive conditions, 6 in highly oxidative conditions, separated by 6 purges under N₂ flow. In a non-laboratory practical application of the process, the N₂ feed and purge period would not be necessary, here they were used to facilitate investigation of the chemical processes involved by determining the elemental balances concerned

Experiments with 80 g of catalyst

Eighty grams of the catalyst almost filled the reformer reactor volume. The set reactor temperature during the WCO/steam/N₂ feed was chosen at 600 °C. This was a compromise between operating on the lower temperature limit of the catalyst's activity and attempting to

minimise the reverse water gas shift reaction for maximum CO₂ and H₂ yield. This was because the full chemical looping reforming process which includes in-situ CO₂ capture should be able to operate in the absence of downstream water gas shift reactors once a CO₂ sorbent is introduced in the reformer. However, the air feed set temperature was chosen at 650 °C in these experiments so that the expected exotherms from the R4-R6 oxidation reactions were able to reach above 850 °C for a sufficient period of time in order to calcine a carbonate if it were present, thereby regenerating it for the following loop.

Figure 2 shows typical gas compositions representative of the 6 cycles, in the form of dry gas concentrations obtained in the second cycle for the first fuel/steam/N₂ feed, therefore starting from the air-oxidised catalyst load. An initial ‘dead time’ of ca. 500 s where hardly any output gases were measured preceded the steady state. This period is the delay between the time at which the valves opened to let the liquid reactants flow and the time at which the product gases first reached the analysers. The steady state was established quickly following this dead time, yielding 47 % H₂, 20% CO₂, 5% CH₄ and 2% CO, and the balance to 100% was assumed to be the N₂ diluent. This assumption was verified by the off-line GC-FID analysis which revealed that methane was the only hydrocarbon formed. When normalising the H₂ concentration for zero nitrogen content, as a practical setting would have, the H₂ volume concentration was 64%. A temperature drop of 40 °C occurred in the reactor simultaneous to reaching the steady state.

Figure 3 shows the unprocessed dry gas measurements under the air feed step of the 2nd cycle. Despite the dry gases concentrations having returned to zero at the end of the N₂ purge period, as soon as the larger air feed of 2000 cm³ min⁻¹ STP started, a final gas products flushing stage initiated as a result of the pressure change, since the N₂ purge had been conducted at the lower rate of 600 cm³ min⁻¹. This was evidenced by two peaks of same shape and duration for H₂ and CH₄ during the initial 240 s, which could only have been

produced under the previous fuel/steam/N₂ step of the same cycle and were thus flushed by the higher air flow. The CO and CO₂ profiles during the air feed indicate that, unlike H₂ and CH₄, they were being produced by the chemical reactions R4-6. The final stage of the reactive period under air feed was signalled by the sharp rise of the O₂ concentration from 0 to 18% at 700 s, just short of the 21% from air due to residual CO₂. The mid-reactor temperature is also plotted in Fig. 3 and clearly shows when the exothermicity of R4-6 resulted in the temperature exceeding the set point of 650 °C. As was intended, a significant period of time (approx. 60 s) was achieved for which the reactor temperature reached above 850 °C, and during which a Ca-based sorbent would have regenerated by calcination, had it been present. The temperature peaked briefly at 1040 °C. This would have a deleterious effect on the catalyst and sorbent for a prolonged period of time, causing sintering. However, in practice, in the presence of a saturated Ca-based CO₂ sorbent at the start of the air feed, the endothermicity of the sorbent calcination would prevent such a damaging temperature to be reached. Conversely, under the fuel/steam/N₂ feed, the carbonation of the sorbent would reduce or even cancel the overall endothermicity in the reformer. Thus, the conditions studied here were artificially adverse to the long term use of the oxygen transfer Ni-catalyst due to the absence of the CO₂-sorbent.

Figure 4 plots $\dot{n}_{Ni \rightarrow NiO}$ calculated using Eq. 5, the rate at which nickel in the catalyst was oxidised, during the air feed just preceding the WCO/steam/N₂ feed of Fig. 2, therefore corresponding to the first cycle. Figure 4 also includes the % Ni oxidation resulting from integrating $\dot{n}_{Ni \rightarrow NiO}$ over time. As Eqs.(4-5) were only valid outside of the flushing period (beyond 200 s, for this first cycle), an extrapolation of the Ni oxidation rate down to zero time was necessary. This was helped by the fact that $\dot{n}_{Ni \rightarrow NiO}$ increased linearly from the end of the flushing time until a peak at 530 s, and therefore a linear interpolation could be applied between 200 and 530 s and for the extrapolation down to zero time. This method was

successfully used for 5 of the 6 air feed steps of the looping experiments at 80 g. The last cycle did not allow this treatment due to the flushing of H₂ and CH₄ from the previous step that carried on for the whole duration of the air feed, making it impossible to identify a period of time where Eqs (4-5) would be valid. In the case of the air feed of the first cycle shown in Fig. 4, the method was validated by finding a % Ni oxidation plateauing at 100%, as was expected for a fresh catalyst. Not shown are $SEL_{NiO\text{ or }CO\text{ or }CO_2}$ the oxygen-containing products selectivities during the period of clear chemical reactivity. For the first cycle (Fig. 4), no CO was detected. In contrast, the second cycle indicated there was significant CO in the products (Fig. 3). The remaining selectivities of the O-containing products CO₂ and NiO for the first cycle began at 50% following the residual flushing of H₂ and CH₄, and ended with 89% NiO and 11% CO₂. These results indicated that the temperature peaks recorded in the reactor could not be attributed to just one of the exothermic reactions (carbon vs. nickel) at any given time during the air feed, but that the oxidation of nickel became gradually predominant. CO appeared as a product as the complete initial oxidation of carbon deposits to CO₂ and of the Ni would have quickly consumed most of the oxygen provided by the finite air feed rate, and created oxygen deprived conditions, leading to incomplete carbon oxidation to CO. As the carbon deposits depleted, more of the oxygen feed was available for the return of complete carbon oxidation to CO₂, ending with the oxidation mechanism being dominated by Ni oxidation and little residual carbon burning.

An equivalent $\dot{n}_{NiO \rightarrow Ni}$ calculation of NiO reduction to Ni using Eq. (3) during the WCO/steam/N₂ feed steps was carried out for each of the 6 cycles, a typical example of which is shown in Fig. 5 for the second cycle (same conditions as Fig. 2). With Eq.(3) containing more terms than its counterpart for the air feed Eq. (5), it was to be expected that the residual error in the rate reached at steady state would also be larger (1×10^{-4} compared to 0.7×10^{-4} mol s⁻¹). This steady state rate could be identified as a residual error as there was a

finite amount of Ni in the reactor able to oxidise. The integration of the rate was therefore limited to the period of time prior to reaching the residual error, and the resulting % NiO reduction to Ni was deemed an underestimate. Figure 5 shows this conversion for the second cycle and indicates 63% upon reaching steady state. This method was successfully used for cycles 2, 4, 5 and 6, the first cycle missing because the catalyst had been reduced by H₂, and the integration for the 3rd cycle missing due to the lack of an observed distinct peak of reduction prior to reaching the steady state.

Table 2 lists the results of the chemical looping reforming experiment for 80 g of catalyst reactor load. Each cycle was defined as two reactive steps, resulting in odd step numbers (1, 3, 5, 7, 9, 11) representing WCO/steam/N₂ feeds and even step numbers (2, 4, 6, 8, 10, 12) for their alternate air feeds. The results include the WCO and steam fractional conversions at steady state and their equilibrium values calculated at the mid reactor temperatures for the odd number steps. WCO and steam conversions were rather constant with repeated cycles and did not seem to deteriorate, despite variations from cycle to cycle. Encouragingly, the last cycle even yielded the best WCO and steam fractional conversions (1 and 0.27 respectively), closest to their estimated equilibrium values (1 and 0.37). Selectivities of the carbon-containing products CO, CO₂ and CH₄ are also listed in Table 2. The significance of CH₄ is that it was the only by-product containing hydrogen and therefore was responsible for lowering the H₂ purity yield (average of 93.8%, calculated with Eq. (6)). One can see that the CO₂ selectivity was very close to the equilibrium value of ca. 70% for the cycles 1, 5 and 6, and exceeded the equilibrium by 10% points for the remainder. Figure 6 shows the extent of NiO conversion to Ni (in %) under the fuel/steam/N₂ feed steps and the extent of Ni conversion to NiO under the air feed steps. Starting from 100% Ni to NiO conversion, the following cycles under air feed saw this decrease to 91 % and 76%, but then recover to 100% for cycle 4 and decrease to 64% for cycle 5. Comparing with the cyclic NiO to Ni

conversions under WCO/steam/N₂ feed steps, these were lower (as expected) than the Ni to NiO conversions due to the larger error-carrying calculation from Eq. (3). However, an overall picture emerged where the two curves seemed to follow each other's ups and downs, which was not incompatible with the ideal situation where they ought to mirror each other in order to be sustained over many cycles. In addition, the difference between Ni to NiO and NiO to Ni conversion from cycle to cycle would have reduced when taking into account the amount of NiO reduced during the N₂ purge period through the carbon eliminating surface reactions R7-8. Despite the uncertainties in the calculation of the extent of NiO reduced to Ni during a cycle, the process certainly looked promising. Based on the air feed steps, the extent of Ni conversion to NiO indicate a fluctuating trend. Experimental conditions such as better reactor temperature control could address the issues of eliminating the CH₄ by-product and obtaining conditions better approaching equilibrium. This, in turn, would diminish the role of carbon oxidation during N₂ and air feeds and favour the oxidation of the Ni catalyst, resulting in a more predictable reactive surface and heat release rate.

Experiments with 40 g catalyst

Experiments with 40 g catalyst load (WHSV of 5.28 hr⁻¹) were also carried out, mainly to provide means of comparison when the sorbent would be incorporated in the reactor load. The fuel and steam conversions as well as C-products selectivities and their calculated equilibrium counterparts are listed in Table 3. The fuel conversion fraction was found to be poor, with an average of 0.2 over the 6 cycles and, consequently, so was the fractional steam conversion, with an average 0.06, indicating conditions far from equilibrium. In contrast, the selectivity of the carbon-containing products was close to equilibrium. This resulted in an average H₂ purity yield of 98% over the 6 cycles indicating a H₂ concentration very close to the ideal. The extent of Ni conversion to NiO under air feed steps and the extent of NiO conversion to Ni under the WCO/steam/N₂ feed steps are plotted in Fig. 6 alongside those

obtained for the 80 g reactor load. The two curves followed each other's oscillations, with Ni to NiO conversions in the 60-100% range and the NiO to Ni conversions in the 60-80% range, similarly to those obtained for the 80 g reactor load. There may be an interesting self-regulating effect which would explain how low extents of O transfer during an air feed step can be followed by high O transfer during the next air step, yielding an oscillating behaviour, but this would have to be investigated with additional experimental methods such as XRD analysis after each cycle to support the respective NiO/Ni amounts estimated by integrating the rates from the O balance equations under both feeds. Overall, the chemical looping behaviour of the Ni catalyst in waste cooking oil steam reforming conditions appeared repeatable for low fuel conversion conditions (ca 0.2) to near complete fuel conversion (0.74-1), representing very coking to less coking conditions, and indicating a robust process.

Conclusions

Waste cooking rapeseed oil can be used successfully as reductant of a Ni-catalyst for steam to carbon ratios from fuel rich (1.73) to excess-steam (4). The S:C of 4, used with a WHSV of 2.64 hr^{-1} , yielded consistently high fuel and steam conversions, close to the calculated thermodynamic equilibrium values. Chemical looping reforming for 6 cycles at S:C of 4 saw some fluctuations in fractional fuel conversion that were mirrored in the steam conversion, but showed steady CO, CO₂ and CH₄ selectivity. The Ni catalyst was able to undergo 6 redox cycles without significant change in conversion or performance deterioration.

Acknowledgments

Our thanks to the Engineering and Physical Research Science Council (EPSRC) for grant EP/D078199/1, to Johnson Matthey for materials, and to E. Knight for the experiments at steam to carbon ratio of 1.73.

References

- Bezergianni, S., Voutetakis, S., and Kalogianni, A., 2009. Catalytic hydrocracking of fresh and used cooking oil. *Ind. Eng. Chem. Res.*, 48, 8402–8406
- Canakci, M., Van Gerpen, J., 2003. A pilot plant to produce biodiesel from high free fatty acid feedstocks. *Transactions of the American Society of Agricultural Engineers* 46 (4), 945–954.
- Canakci, M. The potential of restaurant waste lipids as biodiesel feedstocks. *Bioresour. Technol.* 2007, 98, 183–190
- Chang, S.S., R.J. Peterson, C.T. Ho, in: M.K. Supton (Ed.), *Lipids as a source of flavor*, ACS Symposium Series, vol. 75, ACS, D.C., 1978, p. 18.
- Chen, H.S, Zhang, T., Dou, B., Dupont, V., Williams, P. T., Ghadiri, M., and Ding, Y. , 2009. Thermodynamic analyses of adsorption enhanced steam reforming of glycerol for hydrogen production. *Int. J. Hydrogen Energy*, 34, 7208-7222.
- Czernik, S.; French, R. J.; Magrini-Bair, K. A.; Chornet, E., 2004. *Energy Fuels*, 18, 1738-1743.
- Dou, B., Dupont, V., Rickett, R., Blakeman, N., Williams, P. T., Chen, H., Ding, Y., Ghadiri, M., 2009. Hydrogen production by sorption-enhanced steam reforming of glycerol. *Bioresour. Technol.*, 100, 3540-3547
- Dupont, V., Ross, A. B., Hanley, I., Twigg, M. V., 2007. Unmixed Steam Reforming of Methane and Sunflower Oil: A Single-Reactor Process for H₂-rich Gas. *Int. J. Hydrogen Energy*, 32, 67-79
- Dupont, V., A. B. Ross, E. Knight, I. Hanley, M. V. Twigg, 2008. Production of hydrogen by unmixed steam reforming of methane. *Chem. Eng. Sci.*, 63, 2966-2979.

- Eder, K, and Brandsch, C., 2002. The effect of fatty acid composition of rapeseed oil on plasma lipids and oxidative stability of low-density lipoproteins in cholesterol-fed hamsters. *Eur. J. Lipid Sci. Technol.*, 104, 3-13.
- Fennema, O. R., *Food Chemistry*, 7th edn., Marcel Dekker, New York, 1985
- Gornay, J. , Coniglio, L, Billaud, F. and Wild, G. , in press. Steam Cracking and Steam Reforming of Waste Cooking Oil in a Tubular Stainless Steel Reactor with Wall Effects. *Energy Fuels*, DOI:10.1021/ef900529n.
- Idem, R. O., Katikaneni, S. P. R., Bakhshi, N. N., 1996. Thermal cracking of canola oil: reaction products in the presence and absence of steam. *Energy Fuels*, 10, 1150-1162.
- Kee, R.J., Miller, J.A., Jefferson, T.H., 1980. CHEMKIN: a general purpose problem-independent, transportable, FORTRAN Chemical Kinetics Code Package. Sandia National Laboratories. Report SAND80-8003.
- Kumar, R.V., Cole, J. A., and Lyon, R. K.,1999. Unmixed reforming: an advanced steam reforming process. Preprints of Symposia, 218th. ACS National Meeting, August 22–26, New Orleans, LA, vol. 44, no. 4, pp. 894–898.
- Lutz, A.E.; Rupley, F.M.; Kee, R.J. 1999, *EQUIL: a Program for Computing Chemical Equilibria. CHEMKIN Collection, Release 3.5*; Reaction Design, Inc: SanDiego, pp 2-20.
- Lyon, R.K., J. A. Cole, 2000. Unmixed combustion: an alternative to fire. *Combust. Flame*, 121, 249-261
- Maher, K. D., and Bressler, D. C., 2007. Pyrolysis of triglyceride materials for the production of renewable fuels and chemicals. *Bioresour. Technol.* 98, (12), 2351-2368.
- Marquevich, M., Coll, R., Montane, D., 2000. Steam reforming of sunflower oil for hydrogen production. *Ind. Eng. Chem. Res.* 39, 2140-2147.

- Marquevich, M, Farriol, X., Medina, F., Montane D., 2001. Hydrogen production by steam reforming of vegetable oils using nickel based catalysts. *Ind. Eng. Chem. Res.*, 40, 4757-4766
- Osmont, A., Catoire, L., Gokalp, I., 2007. Thermochemistry of methyl and ethyl esters from vegetable oils. *Int. J. Chem. Kinet.* 39(9), 481-491.
- Prasad, Y.S., and Bakhshi, N. N. 1985. Effect of pretreatment of HZSM-5 catalyst on its performance in canola oil upgrading. *Appl. Catal.* 18, 71–85.
- Tomasevic, A., V. and Siler-Marinkovic, S. S., 2003. Methanolysis of used frying oil. *Fuel Process. Technol.*, 81, 1-6

Table 1 WCO and steam fractional conversions compared to equilibrium calculated values, and molar production rates of CO, CO₂, CH₄ and H₂ obtained experimentally at steady state over (i) reduced and (ii) oxidised catalyst at a set reactor temperature of 700 °C. Rates \dot{n}_i are in $\mu\text{mol/s}$. For all experiments, the molar input rate of carbon was $\dot{n}_{C,in} = 526 \mu\text{mol s}^{-1}$

S/C	X_{WCO} Exp	X_{RSO} Eq. Calc.	X_{H_2O} Exp	X_{H_2O} Eq. Calc.	$\dot{n}_{CO,out}$ Exp	$\dot{n}_{CO_2,out}$ Exp	$\dot{n}_{CH_4,out}$ Exp	$\sum \dot{n}_{C-prod}$ Exp	$\dot{n}_{H_2,out}$ Exp
H ₂ -reduced Ni catalyst									
1.73	0.219	1	0.175	0.667	20.2	86	0.37	107	259
2.5	0.863	1	0.357	0.530	126	251	76	454	829
4	0.999	1	0.279	0.376	117	376	32.9	526	1069
Air-oxidised Ni catalyst									
1.73	0.346	1	0.245	0.667	51.3	131	2.4	186	412
2.5	0.574	1	0.275	0.530	189	104	8.1	312	653
4	0.933	1	0.275	0.376	115	347	28.5	491	1035

Table 2 Chemical looping reforming outputs under WCO/steam/N₂ feed for 80 g catalyst load at S:C 4 and WHSV of 2.64 hr⁻¹. Reactant conversions (X) are given as fractions, selectivities of CO, CO₂ and CH₄ are %, H₂ concentration is in mol % corrected for zero N₂ content, T_{mid} is in Celsius, H₂ purity yield $\eta_{H_2,pur}$ is in %.

Step	Chemical looping reforming experiments							Thermodynamic equilibrium calculations						
	X WCO	X H ₂ O	Sel CO	Sel CO ₂	Sel CH ₄	H ₂ (0N ₂)	T mid	X WCO	X H ₂ O	Sel CO	Sel CO ₂	Sel CH ₄	H ₂ (0 N ₂)	$\eta_{H_2,pur}$
1	0.89	0.25	7.1	73	20	64.0	571	1	0.37	19	70	5.6	68.7	93.2
3	0.74	0.20	5.4	77	18	63.7	560	1	0.36	17	70	5.4	68.0	93.7
5	0.87	0.25	6.6	79	15	65.2	568	1	0.37	19	70	5.5	68.5	95.2
7	0.79	0.20	6.4	79	14	64.1	552	1	0.36	16	69	5.4	67.4	95.1
9	0.95	0.25	7.9	74	18	63.4	562	1	0.36	18	70	5.5	68.1	93.1
11	1.02	0.27	9.7	73	17	63.5	571	1	0.37	19	70	5.6	68.7	92.4

Table 3 As Table 2, for 40 g catalyst load and WHSV of 5.28 hr⁻¹.

Step	Chemical looping reforming experiments							Thermodynamic equilibrium calculations						
	X WCO	X H ₂ O	Sel CO	Sel CO ₂	Sel CH ₄	H ₂ (0 N ₂)	T mid	X WCO	X H ₂ O	Sel CO	Sel CO ₂	Sel CH ₄	H ₂ (0 N ₂)	$\eta_{H_2,pur}$
1	0.19	0.07	12	86	1.9	70.5	579	1	0.37	21	70	5.6	69.2	101.9
3	0.21	0.07	16	80	3.6	68.9	585	1	0.38	22	70	5.6	69.5	99.1
5	0.20	0.06	20	74	5.1	68.5	585	1	0.38	22	70	5.6	69.5	98.6
7	0.14	0.06	23	70	7.5	67.3	589	1	0.38	23	70	5.6	69.7	96.6
9	0.22	0.05	16	68	16.0	64.8	587	1	0.38	22	70	5.6	69.6	93.1
11	0.20	0.07	23	69	7.4	68.8	591	1	0.38	23	70	5.6	69.8	98.6

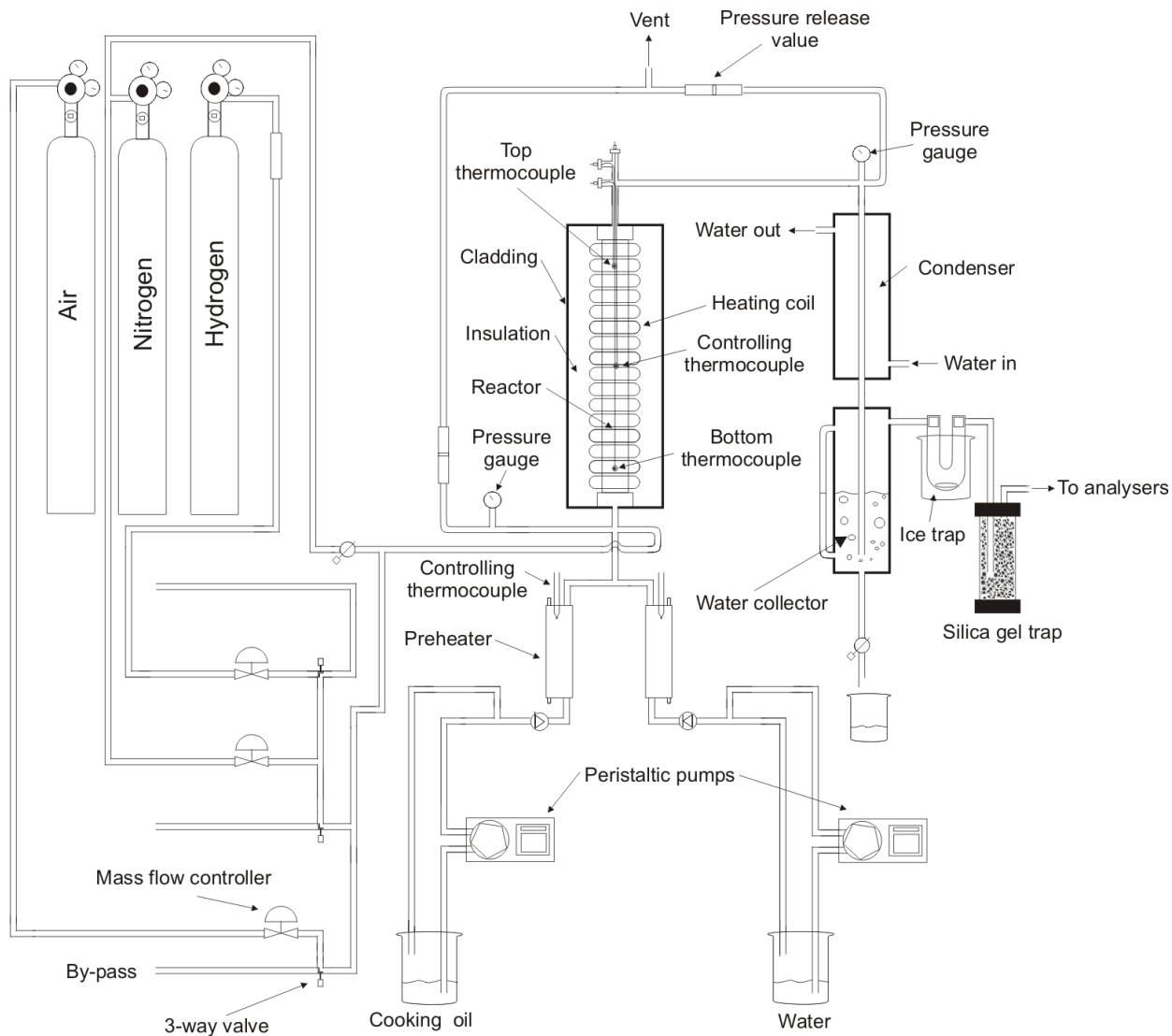


Figure 1 Experimental setup.

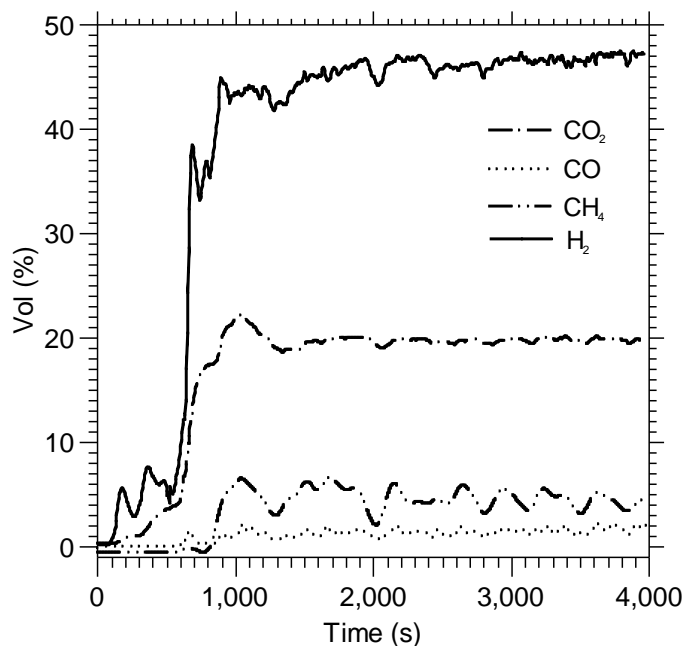


Figure 2 Typical dry gas volume concentrations during the waste cooling oil/steam/N₂ feed (2nd cycle), at S:C of 4, set reactor temperature 600 °C, for 80 g catalyst load. Balance to 100% is the un-measured N₂.

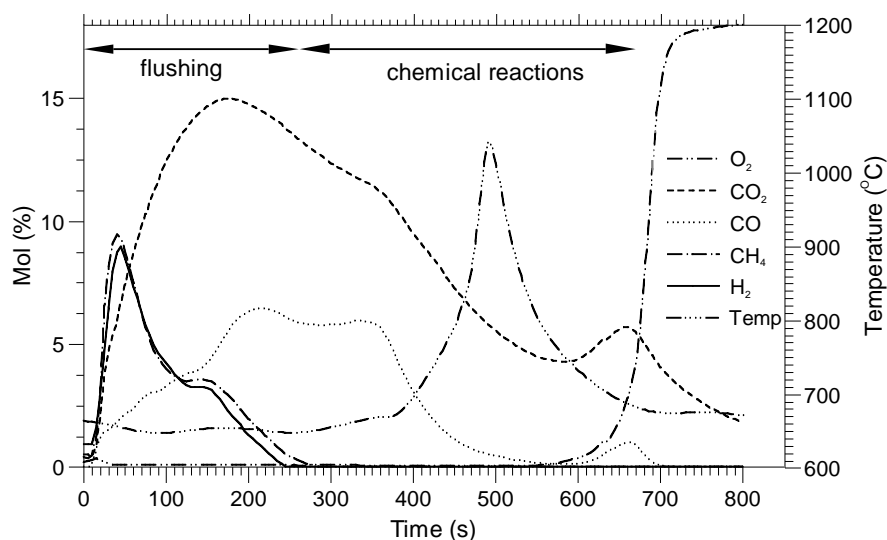


Figure 3 Typical dry gas molar concentrations during a typical air feed step (2nd cycle) following from WCO/steam/N₂ feed step of Fig. 2 (with N₂ purge in between) for 80 g catalyst load and set reactor temperature of 650 °C. The figure also includes the mid-reactor temperature measurement (exotherm of 1040 °C at 500s). The elemental balances outlined in 3.2 are only valid over after the flushing period evidenced by the H₂ and CH₄ residual peaks.

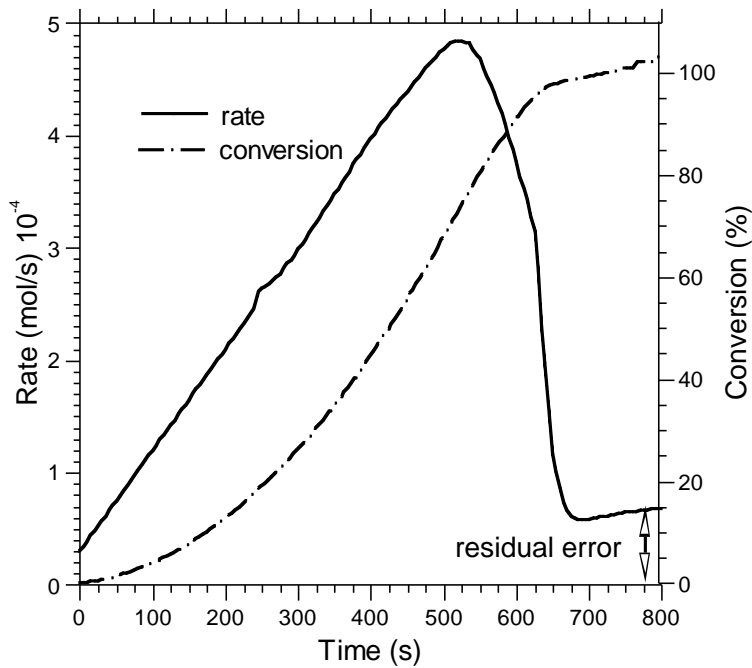


Figure 4. Rate of Ni oxidation to NiO ($\dot{n}_{Ni \rightarrow NiO}$ calculated with Eq. 10) and extent of conversion of Ni to NiO (in %), for cycle 1 under air feed with 80 g catalyst load. Values for the rate prior to 200 s were linearly extrapolated to time zero, corresponding to syngas flushing period.

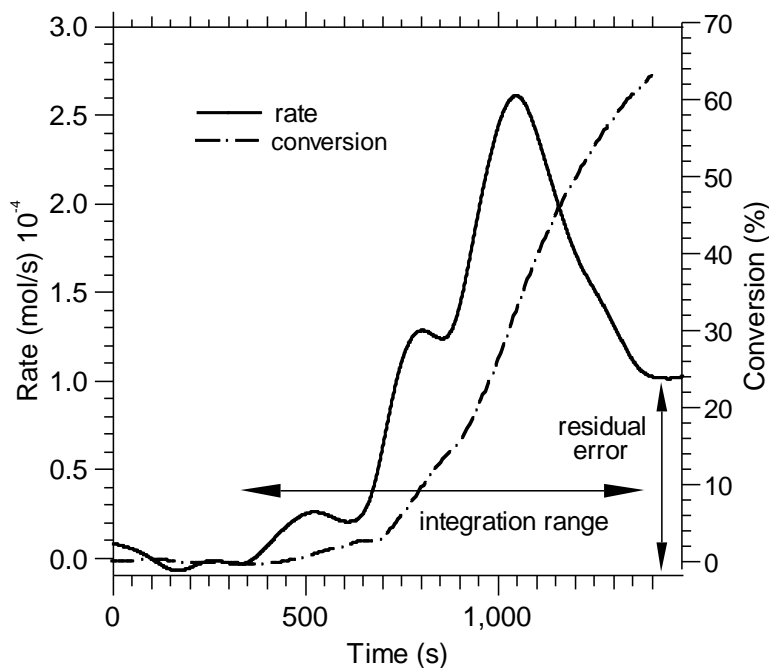


Figure 5 Rate of NiO reduction to Ni ($\dot{n}_{NiO \rightarrow Ni}$ from Eq. 7) during WCO/steam/ N_2 step of cycle 2 (experiment of Fig. 2, 80 g catalyst load), and extent of NiO conversion to Ni (in %) by integration of $\dot{n}_{NiO \rightarrow Ni}$ over time preceding the steady-state residual error.

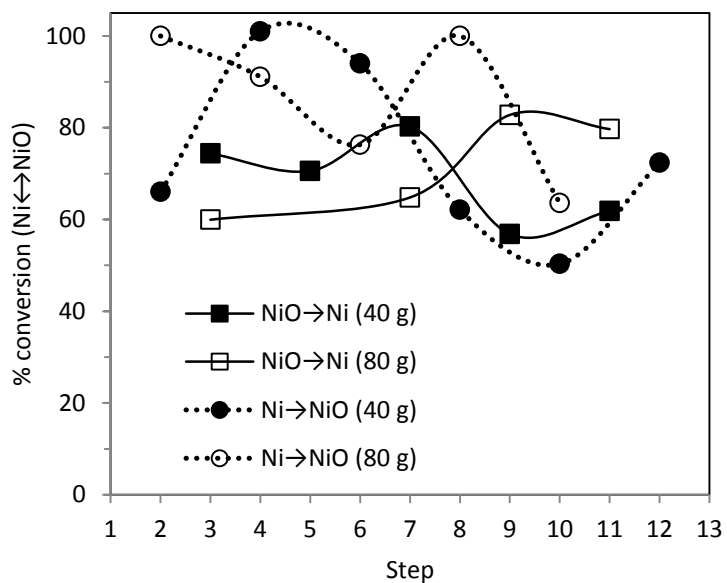


Figure 6 Extent of NiO to Ni conversion during the WCO/steam/N₂ steps and extent of Ni to NiO conversion during the air feed steps for the six cycles carried out with 40 g and 80 g catalyst loads.